In Situ Monitoring of the NaCl + HNO_3 Surface Reaction: The Observation of Mobile Surface Strings

Christopher D. Zangmeister and Jeanne E. Pemberton*

Department of Chemistry, University of Arizona, Tucson, Arizona 85721

Received: July 8, 1998; In Final Form: August 24, 1998

The reaction of single-crystal NaCl(100) with dry HNO_3 was monitored using atomic force microscopy in contact mode. Initial exposure to dry HNO_3 results in the growth of a two-dimensional metastable layer of $NaNO_3$ to nearly complete surface coverage. Exposure of this metastable $NaNO_3$ layer to small amounts of H_2O produces deliquescence of the surface with concomitant rearrangement of the $NaNO_3$ adlayer to form unusual mobile "strings" presumed to contain $NaNO_3$. These strings are transient and eventually crystallize to form rhombohedral $NaNO_3$ crystals sitting on top of the NaCl surface.

Reactions of particulate NaCl formed from evaporated sea salt aerosols with nitrogen oxides have received considerable attention in recent years owing to potential terrestrial atmospheric implications for the formation of reactive chlorinated species.[1−10] These NaCl particles undergo heterogeneous reactions with trace gases to form products that are Cl^- deficient.[11] The formation of gaseous HCl in the terrestrial atmosphere has been hypothesized to be linked to such reactions.[12]

One such reaction is that of vapor-phase HNO_3 with NaCl as shown below:

$$HNO_3(g) + NaCl(s) \rightarrow NaNO_3(s) + HCl(g) \qquad (1)$$

The mechanism and kinetics of reaction 1 have been extensively studied,[1,4,7,8,10] and it has been shown that the reaction probability is increased by the presence of surface defects and adsorbed H_2O.[1,4,7−10] H_2O adlayers allow dissolution of the surface to form a saturated NaCl solution (surface deliquescence) into which HNO_3 can diffuse and react.

Previous work has shown that upon exposure of NaCl to HNO_3, a layer of 1−2 monolayers of $NaNO_3$ caps the surface, thereby protecting it from further reaction.[8,9] Upon addition of H_2O, the surface rearranges to form crystals of $NaNO_3$ sitting on top of the NaCl, exposing fresh NaCl that reacts further with HNO_3.[1,4,7−9] X-ray photoelectron spectroscopy (XPS) results indicate that upon exposure of this surface to H_2O at relative humidities (RH) well below the deliquescence point of NaCl, ca. 80% of the surface becomes fresh NaCl after this $NaNO_3$ rearrangement.[8,9] The remaining 20% of the surface is comprised of rhombohedral $NaNO_3$ crystals[8] as shown by transmission electron microscopy.[9]

The reaction of single-crystal NaCl(100) with dry HNO_3 vapor using contact atomic force microscopy (AFM) is reported here with the goal of better elucidating the mechanism of $NaNO_3$ crystal growth. This reaction is attractive for study, because its reaction kinetics are compatible with AFM imaging times and control of HNO_3 and H_2O exposure is readily achieved.

A Digital Instruments Nanoscope IIIa AFM in contact mode was used for these experiments. Previous work has shown that contact AFM is not destructive to either NaCl or $NaNO_3$ surfaces.[13−15] Calibrated aliquots of dry HNO_3 headspace[1] over a HNO_3/H_2SO_4 solution or saturated H_2O headspace over liquid H_2O were delivered via syringe injections to a glass gastight AFM cell (Digital Instruments, model FC) containing a NaCl-(100) crystal (International Crystal Laboratories.) On the basis of the geometric parameters of the gastight AFM cell, the cell volume is estimated to be ca. 8×10^{-2} cm^3 (3×10^{-6} mol at STP). Images were collected in situ as the reaction proceeded using a 2 Hz scan rate to ensure high image quality and fast acquisition times (4 min/image.) The average RH of the ambient air during these experiments was ca. 14 ± 3%. Thus, the NaCl(100) surfaces were not yet covered by a full monolayer of adsorbed H_2O, since it has been shown that, at RH below 30%, H_2O adsorbs as two-dimensional clusters.[16]

Prior to analysis, a 1 cm × 1 cm single-crystal NaCl(100) was freshly cleaved in ambient air and mounted in the gastight cell. Aliquots of dry HNO_3 and H_2O vapor were dosed onto the NaCl surface as appropriate. Although very small amounts of NO_2 and H_2O might be present in the dosed vapor from dissociated HNO_3 vapor, the amounts of these species, if present, are too low to detect by mass spectrometry[7] and are therefore assumed to be negligible. It is further assumed that the uptake of dosed species by the AFM cell walls is negligible. Image acquisition was initiated immediately after dosing.

Three 5 μm × 5 μm AFM images collected prior to and after dry HNO_3 dosing are shown in Figure 1. Figure 1a shows a contact AFM image of freshly cleaved NaCl(100) prior to HNO_3 dosing. Monotomic steps (0.56 nm) are observed across the surface. After the addition of 1 mL of dry HNO_3 (4×10^{-5} mol/cm^3), a metastable $NaNO_3$ layer forms as shown in Figure 1b. For a dose of this volume, a $NaNO_3$ layer caps the NaCl within 4 min producing a surface with several small (ca. 10 nm diameter) chimney-like defects. These structures are hypothesized to be small $NaNO_3$ crystals that appear owing to the presence of small amounts of H_2O adsorbed on the NaCl surface. XPS on a VG ESCALAB MKII using Al Kα excitation confirms the presence of a $NaNO_3$ capping layer at this stage of the reaction sequence. The N 1s and O 1s binding energies are observed at 407.2 and 532.9 eV, respectively, indicative of $NaNO_3$. Subsequent HNO_3 additions result in no further morphological changes after the capping layer is established.

* To whom correspondence should be addressed. Email: pembertn@u.arizona.edu.

10.1021/jp982910x CCC: $15.00
Published on Web 10/16/1998

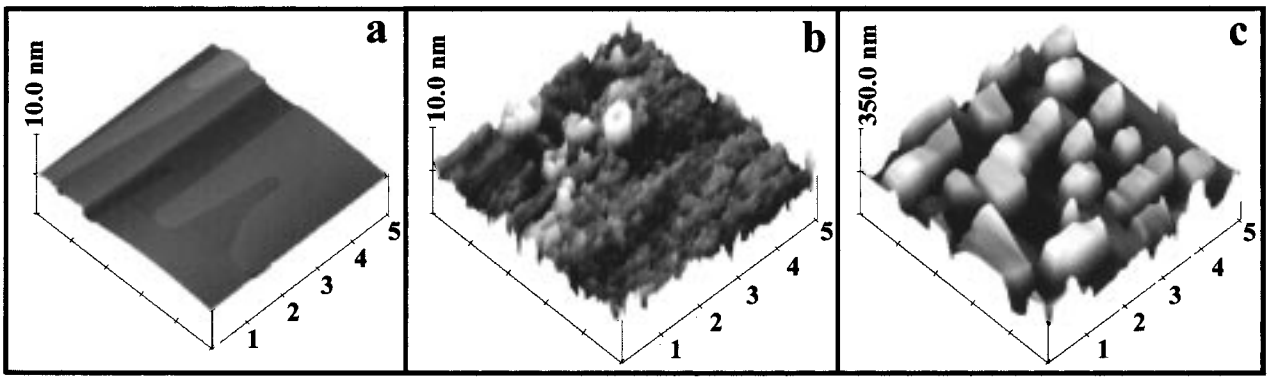

Figure 1. Contact AFM images of (a) NaCl(100) surface prior to HNO_3 exposure; (b) surface in (a) exposed to 4×10^{-5} mol/cm^3 HNO_3; (c) subsequent exposure of surface in (b) to 1×10^{-5} mol/cm^3 H_2O after (a).

TABLE 1: Roughness Analysis Calculations on NaCl(100) as a Function of Exposure

	reactive exposure				
	4×10^{-5} mol/cm^3 HNO_3	4×10^{-5} mol/cm^3 HNO_3 + 1×10^{-5} mol/cm^3 H_2O	9×10^{-5} mol/cm^3 HNO_3 + 1×10^{-5} mol/cm^3 H_2O	1×10^{-4} mol/cm^3 HNO_3 + 4×10^{-5} mol/cm^3 H_2O	1×10^{-4} mol/cm^3 HNO_3 + 1×10^{-4} mol/cm^3 H_2O
total surface area (μm^2)	25.0	26.3	25.5	26.9	27.3
surface area above 2 nm (μm^2)	0.3	6.0	6.6	9.0	12.3
% surface area above 2 nm	1.2	22.7	26.0	33.3	45.2
maximum roughness feature height (nm)	32	136	119	203	244

To study the effect of H_2O exposure on the $NaNO_3$ capping layer, a 1 mL (1×10^{-5} mol/cm^3) H_2O-saturated headspace vapor aliquot was added to the cell resulting in the image shown in Figure 1c. This volume exceeds the cell volume by a factor of ca. 15; therefore, the entire cell volume remains saturated with H_2O vapor throughout the course of these experiments. Upon H_2O addition, the capping $NaNO_3$ layer rearranges to form well-defined $NaNO_3$ "towers" with an average height of ca. 150 nm. These towers are ca. 15 times higher than any of the surface features prior to H_2O exposure (note the *z*-axis scale difference between parts b and c of Figure 1). The regions between the $NaNO_3$ towers appear to be NaCl(100) based on a maximum feature height of ca. 1 nm.

Quantitative determination of the relative proportions of the $NaNO_3$ crystal and unreacted NaCl surface areas from these images was undertaken by conservatively assuming that any area above 2 nm was $NaNO_3$. The results of this analysis are shown in Table 1. Prior to H_2O exposure, only ca. 1% of the surface is above 2 nm in height. After exposure to 1×10^{-5} mol/cm^3 of H_2O, ca. 23% of the surface is composed of $NaNO_3$ crystals. This value is in excellent agreement with previous XPS results, which indicate ca. 20% of the surface as $NaNO_3$ crystals after H_2O exposure.[8]

Additional doses of H_2O and HNO_3 after this $NaNO_3$ crystallization (Figure 1c) result in an increase in coverage and average height of the $NaNO_3$ crystals. This behavior reflects continued reaction of HNO_3 with the exposed NaCl to form crystalline $NaNO_3$ in the presence of adsorbed H_2O. Thus, the presence of a H_2O adlayer facilitates $NaNO_3$ formation. Presumably, $NaNO_3$ formation occurs as a precipitation reaction from saturated solution as opposed to solid-state reaction.[4,6]

A second set of contact AFM experiments was performed to monitor the growth of $NaNO_3$ under lower HNO_3 exposure (ca. 100 times lower exposure than the previous experiments.) Figure 2a shows a 5 μm $\times$ 5 μm image of a freshly cleaved NaCl(100) surface. Prior to HNO_3 exposure, the surface has numerous monatomic steps running ca. 45° to the scan direction. Figure 2b was acquired 2 min after a 10 μL aliquot (4×10^{-7} mol/cm^3) of dry HNO_3 was injected into the gastight cell. The surface roughens with HNO_3 exposure, and the growth of what is presumed to be $NaNO_3$ occurs preferentially along step edges. In addition, small spindles of $NaNO_3$ of ca. 1.2 nm in height (ca. 4 monolayers) grow on terrace sites parallel to the step edges. The surface continues to roughen after 24 min exposure to this single aliquot of 4×10^{-7} mol/cm^3 HNO_3 vapor (Figure 2c). It is important to note that, at this stage of the reaction, the NaCl(100) surface morphology is generally maintained as the reaction proceeds; surface deliquescence due to adsorbed or dosed H_2O has not yet occurred. To achieve nearly complete coverage by $NaNO_3$ (Figure 2d), a total of 40 μL of HNO_3 vapor (1×10^{-6} mol/cm^3) were injected. A cross-sectional analysis of the image in Figure 2d (not shown) indicates a smoother and thinner $NaNO_3$ layer capping the underlying NaCl substrate than observed for larger HNO_3 exposures (Figure 1b), and NaCl step edges are still evident.

Exposure of this surface to 1 mL (1×10^{-5} mol/cm^3) of H_2O-saturated headspace results in the images shown in Figure 3. This H_2O exposure is sufficient to deliquesce the underlying NaCl surface. The NaCl(100) surface morphology evident in Figure 2a−d is replaced by a collection of unusual "strings" presumed to contain $NaNO_3$ unevenly distributed over the NaCl surface. Interestingly, these strings do not follow the previously observed step edges of the NaCl(100) surface (Figure 3a).

A magnified 1 μm $\times$ 1 μm area of Figure 3a is shown in Figure 3b. The $NaNO_3$-containing strings are clearly evident in this presentation and are observed independent of the scan direction. Small (<0.2 nm) roughness features evident in Figure 3b that run parallel to the scan direction are attributed to tip-induced defects. A cross-sectional analysis of this image shown in Figure 4 reveals these strings to be of remarkably consistent height (ca. 1.2 nm) and thickness (ca. 80 nm).

The number of strings and their positions across the NaCl surface change with time. The image in Figure 3c was acquired 4 min after the image in Figure 3a at the exact same spot on the surface. Despite the obvious mobility of these strings, their average height and thickness are maintained. Notable in both images are strings that are very close together yet that do not lead to $NaNO_3$ crystallization.

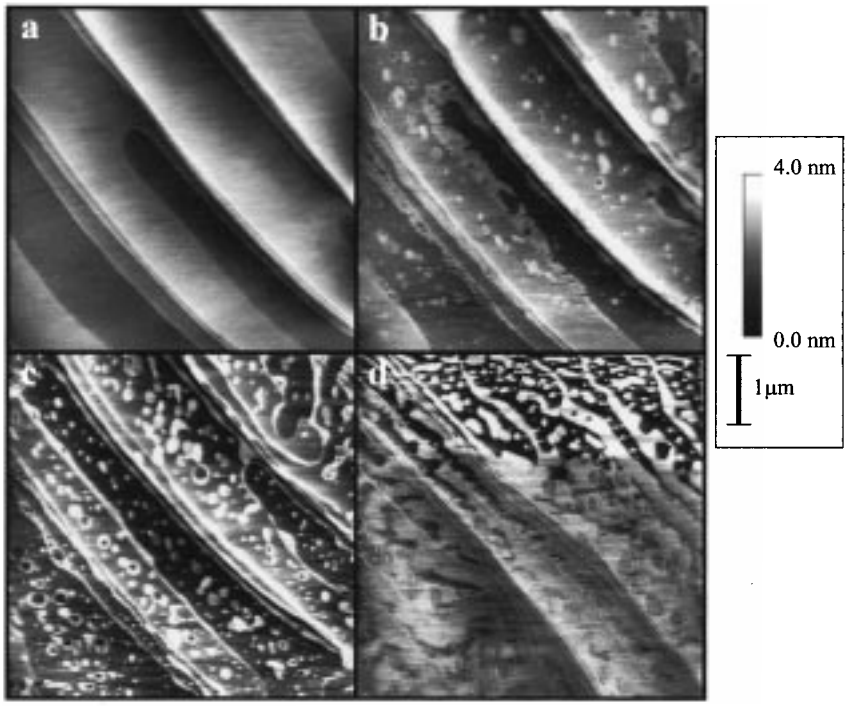

Figure 2. Contact AFM images of (a) NaCl(100) surface prior to HNO_3 exposure; (b) subsequent exposure of surface in (a) to 4×10^{-7} mol/cm^3 dry HNO_3; (c) 24 min after image in (b); (d) subsequent exposure of surface in (c) to an additional 6×10^{-7} mol/cm^3 HNO_3 (total exposure of surface in (a) to 1×10^{-6} mol/cm^3 HNO_3).

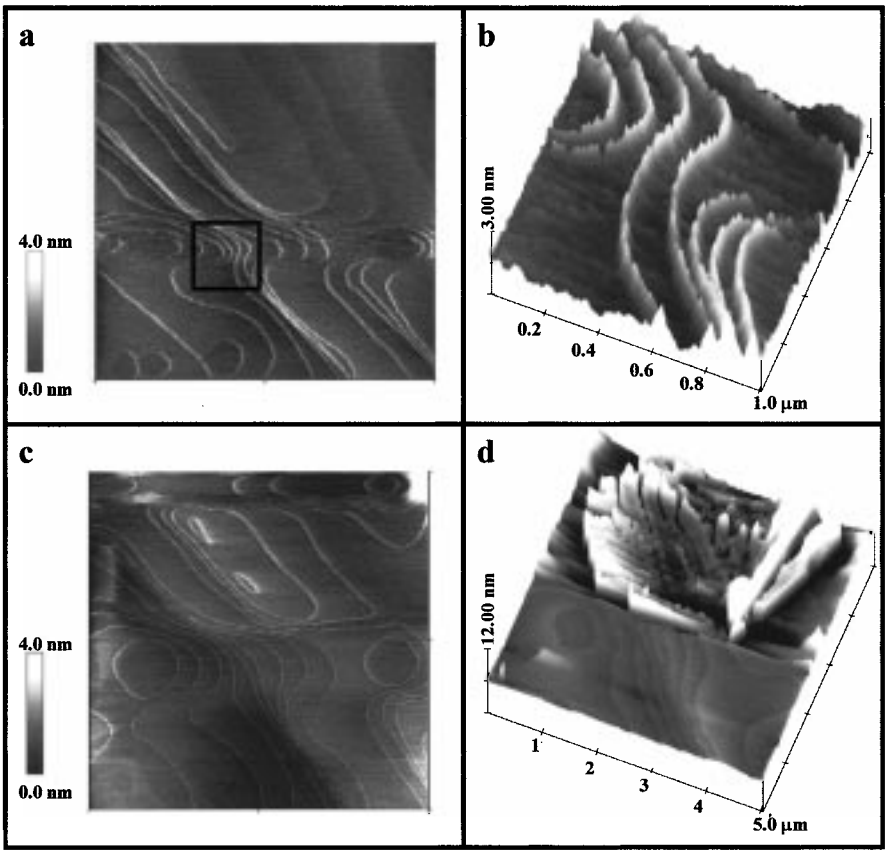

Figure 3. Contact AFM of NaCl(100) surface exposed to 1×10^{-6} mol/cm^3 HNO_3 followed by exposure to 1×10^{-5} mol/cm^3 H_2O. (a) 5 μm $\times$ 5 μm image of $NaNO_3$ strings on NaCl; (b) 1 μm $\times$ 1 μm zoom of boxed region in image (a); (c) 5 μm $\times$ 5 μm image of strings 4 min after image in (a); (d) 5 μm $\times$ 5 μm image after $NaNO_3$ crystallization.

$NaNO_3$ crystallization at this spot on the surface is evident in the image acquired ca. 8 min after this single H_2O exposure. Figure 3d shows one such crystal of ca. 30 nm in height that has apparently formed from the upper area in Figure 3c in which the strings have formed a completely closed pseudo-rectangular arrangement. Significantly, no strings are evident on the surface in the immediate area surrounding the crystal; however, sub-nanometer string "tracks" are observed on the NaCl at positions

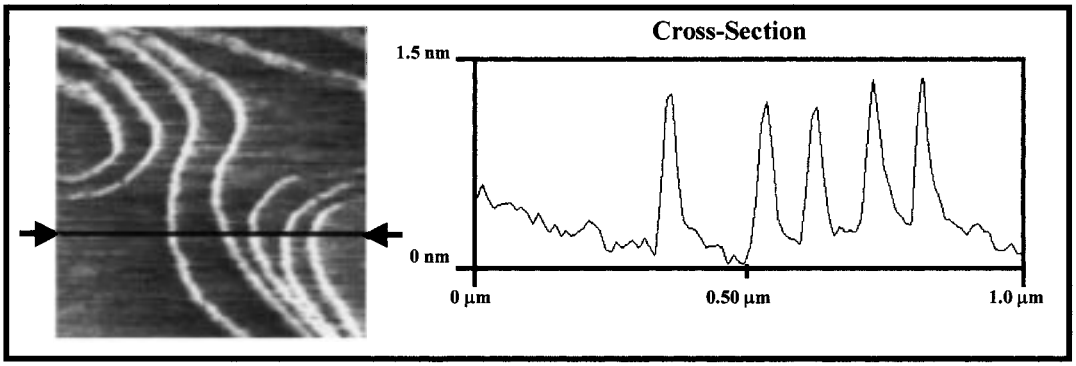

Figure 4. Cross-sectional analysis of $NaNO_3$ strings across the NaCl(100) surface.

where the strings previously existed. At the end of this surface reaction induced by exposure to H_2O, the surface is covered by ca. 30 μm rhombohedral $NaNO_3$ crystals larger than those shown in Figure 1c.

The origin of the strings observed after surface deliquescence is rationalized as follows. Exposure of the $NaNO_3$-capped surface to H_2O results in displacement of the metastable $NaNO_3$ layer with concomitant deliquescence of the underlying NaCl surface, the energetically most favorable process. (The energetics of this system are probably dictated by the lack of a commensurate lattice between $NaNO_3$ and NaCl as ascertained by computer calculations using Epicalc.[17]) The formation of strings containing $NaNO_3$ that are mobile is attributed to the presence of a H_2O adlayer on the NaCl surface and the lack of a strong interaction between $NaNO_3$ and the NaCl surface. The transient nature of these strings suggests a kinetic barrier associated with the crystallization of $NaNO_3$. If $NaNO_3$ crystallization occurs as a precipitation reaction from saturated aqueous solution, then this kinetic barrier could be the dissolution of these strings in the underlying H_2O adlayer.

In summary, contact AFM has been used to observe in situ the reaction of HNO_3 with NaCl. Exposures of NaCl(100) to large amounts of HNO_3 (4×10^{-5} mol/cm^3) with subsequent exposure to H_2O results in a surface containing rhombohedral $NaNO_3$ crystals (ca. 23% of the surface area) with the remaining surface as unreacted NaCl. The newly exposed NaCl surface further reacts with HNO_3 to form additional $NaNO_3$. Images acquired after low HNO_3 exposure (4×10^{-7} mol/cm^3) show $NaNO_3$ growth along NaCl step edges. The $NaNO_3$ layer continues to grow two-dimensionally until complete surface coverage is achieved. Subsequent H_2O exposure results in surface deliquescence and the formation of mobile strings containing $NaNO_3$. These strings are transient in nature with the formation of rhombohedral $NaNO_3$ crystals as the final surface state.

Acknowledgment. The authors gratefully acknowledge support of this research by the National Science Foundation (CHE-9504345.) The authors thank Dr. Andrew Back for computational assistance and useful discussions on the $NaNO_3$/NaCl interface.

References and Notes

(1) Vogt, R.; Finlayson-Pitts, B. J. *J. Phys. Chem.* **1994**, *98*, 3747.
(2) Timonen, R. S.;, Chu, L. T.; Leu, M.; Keyser, L. F. *J. Phys. Chem.* **1994**, *98*, 9509.
(3) Karlsson, R.; Ljungström, E. *J. Aerosol. Sci.* **1995**, *26*, 39.
(4) Leu, M.; Timonen, R. S.; Keyser, L. F.; Yung, Y. Y. *J. Phys. Chem.* **1995**, *99*, 13203.
(5) Caloz, F.; Fenter, F. F.; Rossi, M. J. *J. Phys. Chem.* **1996**, *100*, 7494.
(6) Peters, S. J.; Ewing, G. E. *J. Phys. Chem*, **1996**, *100*, 14093.
(7) Beichert, P.; Finlayson-Pitts, B. J. *J. Phys. Chem.* **1996**, *100*, 15228.
(8) Laux, J. M.; Fister, T. F.; Finlayson-Pitts, B. J.; Hemminger, J. C. *J. Phys. Chem.* **1996**, *100*, 19891.
(9) Allen, H. C.; Laux, A. J. M.; Vogt, R.; Finlayson-Pitts, B. J.; Hemminger, J. C. *J. Phys. Chem.* **1996**, *100*, 6371.
(10) Langer, S.; Pemberton, R. S.; Finlayson-Pitts, B. J. *J. Phys. Chem. A* **1997**, *101*, 1277.
(11) Hitchcock, D. R.; Spiller, L. L.; Wilsson, W. E. *Atmos. Environ.* **1980**, *14*, 165.
(12) Keene, W. C.; Pszenny, A. A. P.; Jacob, D. J.; Duce, R. A.; Galloway, J. N.; Schultz-Tokos, J. J.; Sievering, H.; Boatman, J. F. *Global Biochem. Cycles* **1990**, *4*, 407.
(13) Shindo, H.; Ohashi, M.; Tateishi, O.; Seo, A. *J. Chem. Soc., Faraday Trans.* **1997**, *93*, 1169.
(14) Shindo, H.; Ohashi, M.; Baba, K.; Seo, A. *Surf. Sci.* **1996**, *357*−*358*, 111.
(15) Nakahara, S.; Langford, S. C.; Dickinson, J. T. *Tribol. Lett.* **1995**, *1*, 277.
(16) Peters, S. J.; Ewing, G. E. *Langmuir* **1997**, *13*, 6345.
(17) Last, J. A.; Hiller, A. C.; Hooks, D. E.; Maxson, J. B.; Ward, M. D. *Chem. Mater*. **1998**, *10*, 422.